

# Integrated Thermal and Fabrication Workflow for Structural Frameless Glass Structures

**Gergana Rusenova<sup>a</sup>, Julian Länge<sup>a</sup>, Thiemo Fildhuth<sup>a</sup>, Anna Buksak<sup>b</sup>, Timon Peters<sup>c</sup>,  
Isabell Ayvaz<sup>c</sup>, Matthias Haller<sup>d</sup>, Roman Schieber<sup>a</sup>, Ulrich Knaack<sup>c</sup>**

- a knippershelbig GmbH, Germany, [g.rusenova@knippershelbig.com](mailto:g.rusenova@knippershelbig.com), [j.laenge@knippershelbig.com](mailto:j.laenge@knippershelbig.com), [t.fildhuth@knippershelbig.com](mailto:t.fildhuth@knippershelbig.com), [r.schieber@knippershelbig.com](mailto:r.schieber@knippershelbig.com)
- b Yachtglass GmbH & Co. KG, Germany, [anna.buksak@yachtglass.de](mailto:anna.buksak@yachtglass.de)
- c Technische Universität Darmstadt ISM+D, Germany, [peters@ismd.tu-darmstadt.de](mailto:peters@ismd.tu-darmstadt.de), [ayvaz@ismd.tu-darmstadt.de](mailto:ayvaz@ismd.tu-darmstadt.de), [knaack@ismd.tu-darmstadt.de](mailto:knaack@ismd.tu-darmstadt.de)
- d Solutia Deutschland GmbH, Germany, [mmhall@eastman.com](mailto:mmhall@eastman.com)

## Abstract

For more than two decades, glass shell structures have shaped architecture for their transparency and strength, traditionally using steel lattices with non-load-bearing glass. This project explores fully glass-based envelopes without conventional profiles. It investigates frameless constructions with laminated steel fittings between panes, enabling glass as a load-bearing, thermally effective envelope. Methods combine thermal simulations, structural detailing, and parametric automation. A novel linear fitting system for insulating glass was refined through iterative prototyping, laser welding, and tolerance strategies. Fabrication challenges underscored the need for tighter design-manufacturing coordination. Thermal simulations across five climate zones informed a custom visual programming tool for interactive temperature analysis and design guidance. The parametric workflow automates geometry, fabrication data, and assembly logic for applications from façades to yacht canopies. A full-scale Glasstec 2024 mock-up demonstrated both potential and fabrication sensitivity, highlighting the importance of iterative, feedback-driven development in frameless glass architecture.

## Keywords

Frameless Load-bearing Glass, Transparent Structural Connection, CO<sub>2</sub> Emission Reduction, Thermal Simulations, Parametric Workflow

## Article Information

- Digital Object Identifier (DOI): [10.47982/cgc.10.678](https://doi.org/10.47982/cgc.10.678)
- Published by [Challenging Glass](#), on behalf of the author(s), at [Stichting OpenAccess](#).
- Published as part of the peer-reviewed [Challenging Glass Conference Proceedings](#), Volume 10, June 2026, [10.47982/cgc.10](https://doi.org/10.47982/cgc.10)
- Editors: Christian Louter, Freek Bos & Jan Belis
- This work is licensed under a [Creative Commons Attribution 4.0 International](#) (CC BY 4.0) license.
- Copyright © 2026 with the author(s)

## 1. Introduction

Natural daylight plays a key role in human comfort and well-being, making glass roofs and façades a central element of contemporary architecture. Their ability to maximize transparency and daylight penetration has driven widespread use in public buildings, offices, and maritime applications such as yacht canopies. In Germany, the flat glass market reached €1.4 billion in 2025, largely fueled by façades and curtain walls (Salim, 2025), while the European luxury yacht market is projected to grow from €5.4 billion in 2025 to €9.0 billion by 2030 (Intelligence, 2025). Despite this growth, many existing systems depend on heavy steel substructures or complex nodes that compromise transparency, thermal performance, and sustainability (see Section 2), highlighting the need for a new structural glass solution.

This research addresses this gap by developing a load-bearing frameless glass envelope suitable for curved roofs up to 10 x 10 m span and transparent yacht canopies without conventional steel substructures. Central to the concept is a novel linear stainless-steel fitting laminated into safety glass, capable of transferring shear and bending stresses between panels. Eliminating bulky steel nodes reduces material use, simplifies assembly, and targets a 50% reduction in CO<sub>2</sub> emissions during fabrication and end-of-life phases compared to traditional steel-glass systems. Automated fabrication workflows are further explored to enhance efficiency, while the architectural design emphasizes minimalism, transparency, and spatial openness.

The research is conducted within the collaborative project Frameless Glass Construction (see Acknowledgements), involving knippershelbig GmbH, Yachtglass GmbH & Co. KG, TU Darmstadt – ISM+D, and Eastman. Each partner contributes specialized expertise in construction development, lamination and assembly, interlayer materials, and structural validation, collectively advancing a fabrication-ready frameless glass system.

While earlier publications focused primarily on structural behaviour (Ayvaz et al., 2025), this paper emphasizes thermal performance, life cycle assessment, and the automation of geometry generation and fabrication. By integrating simulation-driven design with parametric workflows, the research establishes a scalable and environmentally informed approach to frameless glass architecture, underscoring the value of close collaboration between academic research and industry practice.

## 2. Background and related work

Modern architecture increasingly seeks lightness and seamless integration with the environment, leading to glass envelopes with minimal visible fixings. Roof glazing can be realized through various structural systems, each offering distinct aesthetic and technical benefits. The following sections outline the most prominent approaches and their current developments.

### 2.1. Grid Shell Structures

The most common system for overhead glazing is the grid shell—a spatially curved lattice, typically made of steel, that transfers loads through its interconnected members. In these conventional systems, steel transfers the structural forces, while glass remains a passive, non-loadbearing infill. This approach achieves stability but limits the potential of glass as a structural material. Structural glass in buildings—such as thermally toughened soda-lime silicate glass, laminated glass, and tempered glass—exhibits high compressive strength—often cited between 700 and 1000 MPa (N/mm<sup>2</sup>), compared to steel's

200–500 N/mm<sup>2</sup> (European Committee for Standardization (CEN), 2005) — yet its brittleness and low tensile capacity make load-bearing applications complex and risky.

To integrate glass into these systems, panels are usually secured with pressure plates or bonded to auxiliary frames using high-strength silicone adhesives, a technique known as structural glazing. From the exterior, the supporting structure is concealed, leaving only narrow joints between panes, while the interior reveals the steel framework. These designs often push aesthetic boundaries through free-form geometries, as seen in the Chadstone Shopping Centre in Melbourne, which required approximately 70.6 kg of steel per square meter (Seele, 2025). Such projects are highly customized, and demand intricate structural calculations for every individual pane, underscoring the complexity of current grid shell solutions.

Furthermore, cable- and point-supported glazing systems use tensioned cables and minimal steel components to create highly transparent, lightweight glass façades and roofs, as seen in the courtyard roof of the Maximilian Museum (Detail, 2001). Structural glass construction goes a step further by using glass itself as a load-bearing material in beams, fins, and columns, exemplified by projects such as the Apple Store Fifth Avenue Cube (Arch Daily, 2025), though both approaches face challenges related to durability, sealing, and the brittle nature of glass.

## 2.2. Exhibition and Research Projects

Research into structural glass has pushed the boundaries of design and fabrication. A notable concept developed in 2004 at the Institute for Lightweight Structures and Conceptual Design (ILEK), University of Stuttgart, involved an 8.5 m glass shell composed of 44 panels bonded with epoxy resin, eliminating metallic connectors entirely (Sobek & Blandini, 2004). Laminated safety glass combined with chemically pre-stressed glass transferred compression forces into a titanium ring supported by steel columns. Further studies, such as Stefan Marinitsch's dissertation, explored adaptable linear connection details for folded glass structures, using embedded metal components to achieve variable angles and structural flexibility (Marinitsch, 2015).

Another example is the Eastman Frameless Glass Structure, realized by knippershelbig for a virtual live event in 2020. This small-scale prototype (4.5 m × 2.5 m) featured a vertical glass wall with slight cantilevering (knippershelbig, 2025). The laminated glass panels were connected using locally short stainless-steel fittings embedded in multiple layers of translucent PVB interlayer. Unlike a full façade, the design intentionally left open joints, and the load case was limited to moderate compression forces and indoor temperature conditions. All steel connections were CNC-milled, resulting in high precision; however, this approach significantly increased the cost of the prototype, exceeding the market price of comparable solutions. Consequently, a new concept was required to achieve economic feasibility while ensuring the integrity of the thermal envelope. Nevertheless, this prototype served as a critical foundation for the developments presented in this paper and was instrumental in enabling subsequent innovations (Fildhuth, 2022).

## 2.3. Current Limitations and Challenges

The projects discussed in this section reflect ongoing efforts to reduce metal components and improve connection technologies for more transparent and adaptable glass structures. Despite progress, current glass roof systems remain limited by visually dominant steel frames and nodes, which reduce transparency, increase CO<sub>2</sub> emissions, and prevent glass from acting as a load-bearing material. Connection nodes are often labour-intensive, bespoke, and prone to sealing issues.

Individual systems present further drawbacks: cable-supported glazing cannot permanently accommodate insulating glass and has shown long-term leakage; grid shells rely on obstructive steel frameworks, visible welds, and perform poorly under asymmetric loads; and glass beam systems are limited to flat geometries, require large beam depths, and are vulnerable under wind suction. Research prototypes, while innovative, are typically geometry-specific, lack thermal performance, and remain unproven in long-term use. Together, these limitations highlight the need for a solution that unites structural efficiency, aesthetic clarity, and sustainability.

#### 2.4. Proposed Fitting–Foil–Glass Composite (FFGC)

Building on insights from the Eastman Frameless Glass Structure, this project introduces a new Fitting–Foil–Glass Composite (FFGC) system with continuously laminated linear steel fittings and integrated thermal insulation for double- and triple-insulated glazing units. Glass is used as a load-bearing material, enabling spans of up to 10 × 10 m without steel substructures while maintaining high transparency, structural efficiency, and sustainability. A novel linear stainless-steel fitting laminated into safety glass transfers compression, tension, and bending moments between panels, eliminating bulky nodes and reducing steel use and CO<sub>2</sub> emissions by up to 50%. Automated fabrication workflows, adapted lamination processes, and digital identification systems enable efficient production and assembly.

The paper proceeds from the development of the FFGC connection through requirements definition, prototyping, and iterative refinement, to building-physics simulations defining thermal performance limits, parametric workflows for architectural application, and a Life Cycle Assessment quantifying environmental benefits. All methods are validated through a full-scale mock-up presented at Glasstec 2024, demonstrating feasibility under real-world conditions.

### 3. Development of the FFGC System

The development of the FFGC system employed complementary methods applied iteratively throughout the project, including definition of requirements, physical prototyping, and construction development. Implemented at varying stages and levels of detail, these methods reflect the adaptive nature of the research process. Together, they align geometric, fabrication, structural, thermal, and sustainability considerations to achieve a viable and efficient solution.

#### 3.1. Definition of Requirements for the FFGC System

At the start of the Frameless Glass Construction project, the wide range and complexity of design, performance, and fabrication requirements posed a major challenge. To address this systematically, a comprehensive requirements profile was created and continuously updated on a collaborative Microsoft Whiteboard (Fig. 1). The diagram visualized relevant aspects and their interdependencies, organizing parameters into five categories: construction, aesthetics, building physics, structural performance, and production and assembly. Additional considerations included cost efficiency, CO<sub>2</sub> reduction, geometric relationships between global structure and local fittings, and climate-related thermal performance. Quantitative parameters comprised material values and standard-based targets, as well as variables identified for further investigation, while qualitative parameters covered design, performance, and production goals. Early analysis indicated that physical prototyping was a critical first step to evaluate feasibility, cost efficiency, and fabrication precision of the linear fittings.

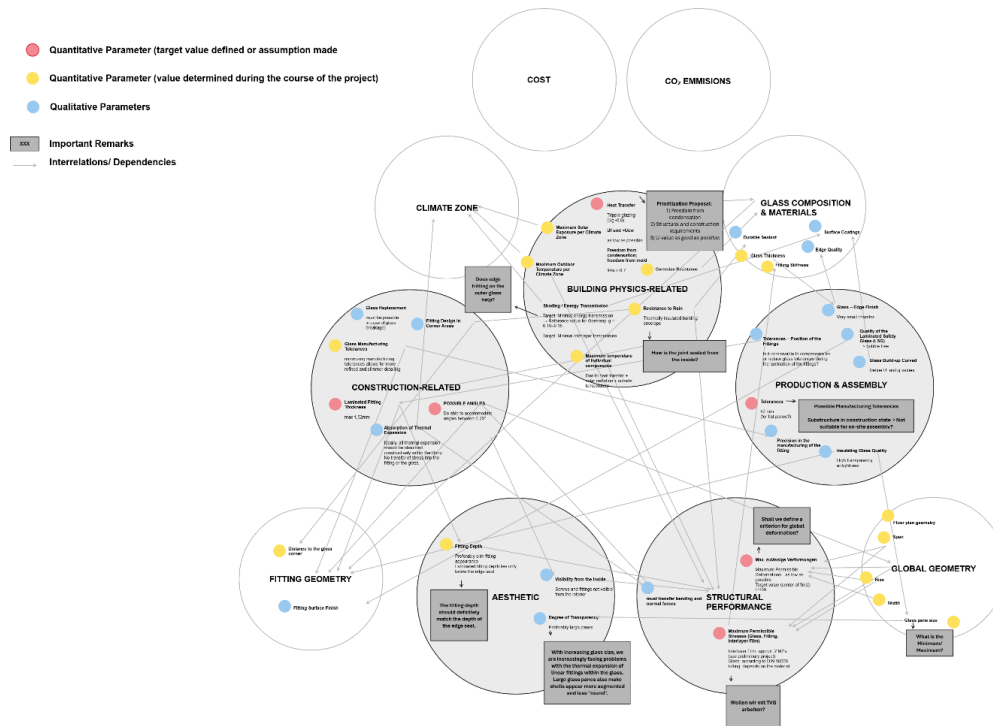


Fig. 1: The requirements profile of the linear fitting as a complex system of interactions between qualitative and quantitative parameters (Source: knippershelbig).

### 3.2. Physical Prototyping as an Integral Design Method

Physical prototyping was conducted continuously throughout the project, beginning at an early stage to directly inform the development of the connection detail. This iterative process enabled validation of design assumptions, assessment of fabrication feasibility, and refinement of the glass and steel fitting geometry under practical constraints. The initial concept was derived from the Eastman Frameless Glass Structure and evolved into a linear fitting laminated along the glass edges within a double-glazed unit, allowing for continuous sealing and compliance with thermal requirements.

Potential manufacturing methods were evaluated in collaboration with four steel construction companies to replace the costly CNC milling used previously. Laser welding, milling, continuous casting, and metal 3D printing were assessed, leading to a market-oriented solution composed of three profiles that were assembled using laser welding, reducing fabrication costs by avoiding single-block machining.

Based on this approach, initial prototypes were produced using detailed shop drawings. The fittings were manufactured externally and laminated into glass units. Key variables included T-profile thickness, lamination depth, and number of PVB layers. The lamination depth was defined to align the fitting flush with the spacer of the double-glazed unit, ensuring transparency and material efficiency. Prototypes ranged from 500 mm samples to fittings up to 2 m long.

While the prototypes validated the fabrication concept at architectural scale, manual laser welding led to quality challenges, particularly deformation, uneven welds, and non-orthogonal joints (see Fig. 2).



Fig. 2: Example of non-orthogonal welding of the flat steel components of the fitting (Source: Yachtglass).

These geometric inaccuracies caused air entrapment during lamination, resulting in bubbles and reduced lamination quality (see Fig. 3), with potential structural implications (see Section 4.2). Despite process optimizations, these issues persisted, indicating the need for further research and closer integration of steel manufacturing expertise in future project phases. This issue remained a topic of investigation throughout the entire project. Further research is clearly required, and integrating a steel manufacturer as part of the core team would be highly beneficial for subsequent project phases.



Fig. 3: Example of laminated non-orthogonal steel fitting (left) and resulting air entrapment (middle and right) (Source: Yachtglass).

### 3.3. Iterative Construction Detail Development

Following the fabrication of the first linear fittings, the next step focused on a detailed investigation of the connection detail, addressing lamination, assembly, thermal insulation, and aesthetic requirements through an iterative collaborative process. This development built on the connection principle of the Eastman Frameless Glass Structure (see Section 1.4), where fitted and oversized holes allow assembly tolerances, with the oversized hole subsequently filled with cement mortar. A CNC-milled component with two boreholes—one for guided filling and one for control—was adopted and

refined, leading to the first complete iteration of the construction detail for a double-glazing unit with linear fittings (see Fig. 4).

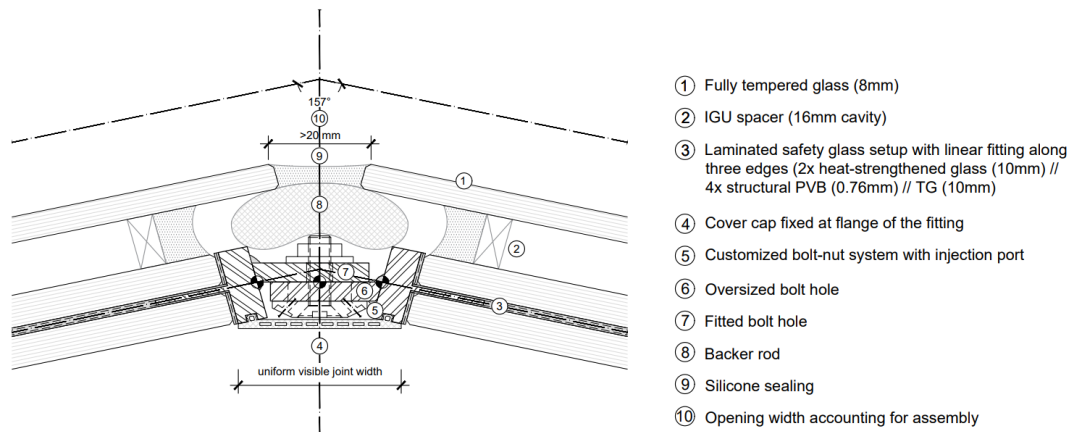


Fig. 4: Initial fully developed iteration of the construction detail (Source: knippershelbig).

The detail was designed for adjacent glass elements meeting at an angle, reflecting the investigation of curved glass roofs and façades to exploit glass as a load-bearing material (see Section 4.2). Joint spacing was carefully analyzed to minimize gaps, reduce material usage, and achieve balanced proportions, while maintaining sufficient load-bearing capacity of the screw connections. To ensure a slim and uniform interior joint, the thickness of the non-laminated fitting section was adjusted to integrate a groove for a continuous interior gasket (Fig. 5, item 4), providing thermal insulation. A backer rod was added to support the exterior silicone seal. For the edge seal between tempered and laminated glass, a ‘warm edge’ solution was developed; following evaluation of steel, aluminum, and plastic spacers, a plastic spacer (Super Spacer® TriSeal Premium) was selected for prototyping due to its lower thermal conductivity.

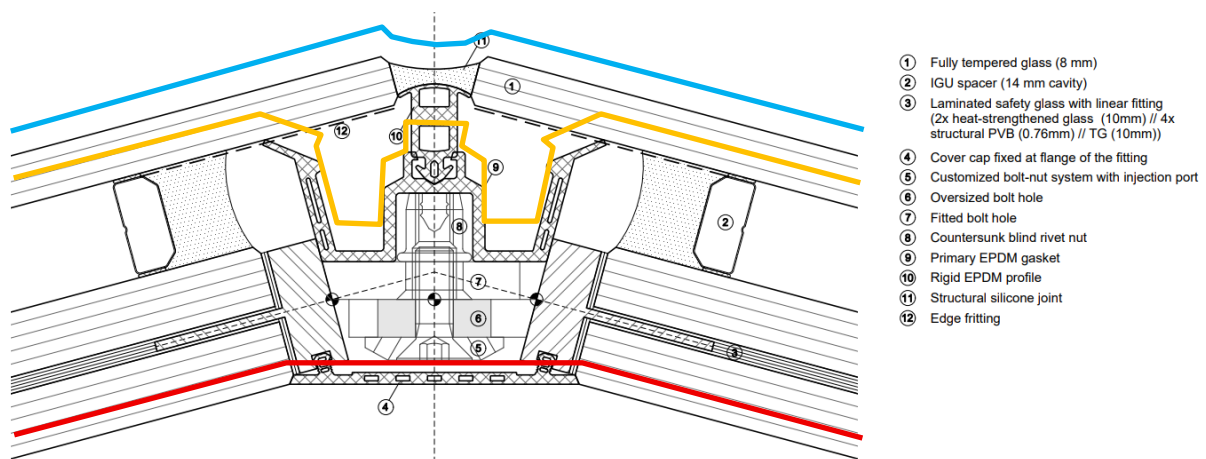


Fig. 5: Final iteration of the construction detail designed for a double-glazing unit (Source: knippershelbig).

The detail was further refined to comply with the three-level sealing principle (DIN EN 13830:2020-11). Two insulating glass units meet at an angle to form the ridge (see Fig. 5), with a continuous outer silicone joint providing weather protection (Fig. 5, item 11, blue line). A recessed blind rivet nut (Fig. 5, item 8) serves as the primary load-bearing element, while an EPDM gasket (Fig. 5, item 9) serves as a secondary drainage layer (Fig. 5 yellow line). A rigid, height-adjustable EPDM support profile replaces

the conventional backer rod (see Fig. 11, item 10), providing uniform support for the silicone joint. On the interior side, a segmented EPDM pressure cap acts as a vapor tight seal (see Fig.5, item 4, red line). Dead load transfer is supported by thermally separated stainless-steel bent components fastened to the linear steel fitting and positioned according to load cases.

Finally, the construction detail was adapted for triple-insulated glazing units by enlarging the EPDM gasket and rigid EPDM profile to accommodate the additional exterior glass pane (see Fig. 6, items 9 and 10).

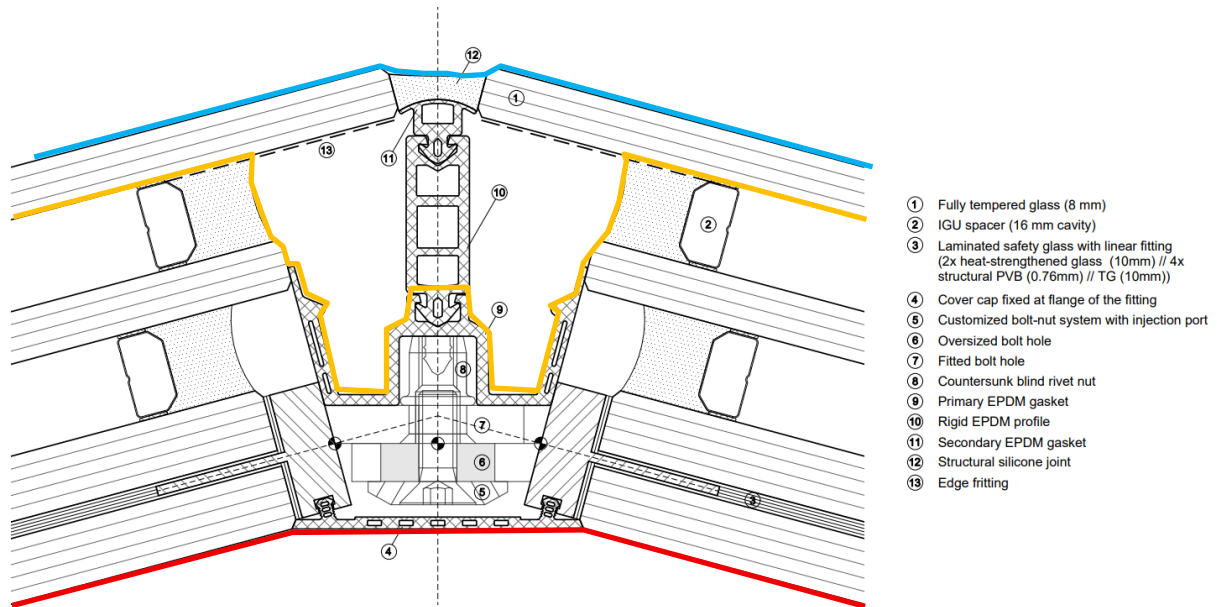


Fig. 6: Final iteration of the construction detail designed for a triple-glazing unit (Source: knippershelbig).

The finalized construction details for both double and triple glazing were subsequently used as input for the building physics simulations described in the following section.

## 4. Building Physics Properties of the FFGC system

### 4.1. Definition of Requirements for the Simulations of the FFGC system

The requirements profile of the FFGC system (see Section 2) defined the scope of the building physics simulations for evaluating the FFGC system. The main objectives were to ensure weatherproof thermal performance across different climate zones—preventing thermal bridges and condensation—and to assess temperature-dependent force transfer through the shear-resistant PVB interlayer, where differential thermal expansion under extreme conditions may cause delamination.

To address these aspects, two simulation tools were used. WINISO was applied to analyze heat transfer, thermal bridging, and condensation risk, providing U-value calculations in compliance with standards such as EN ISO 10077-2. In parallel, the multiphysics FEM software COMSOL was employed to simulate temperature changes due to solar radiation, enabling static and transient analyses of materials with different thermal expansion behavior. U-value and Condensation Risk Assessment using WINISO

For the triple-glazed assembly, the frame U-value ( $U_f$ ) calculated according to EN ISO 10077-2 is  $2.0 \text{ W/m}^2\text{K}$ , which is higher than values typically achieved by market-standard steel façade systems

such as Jansen VISS or Raico THERM+ SI ( $U_f \approx 1.0\text{--}1.5 \text{ W/m}^2\text{K}$ ). This is due to the structural placement of the load-bearing steel profiles within the insulation plane, increasing heat losses. For a representative roof module ( $1.23 \times 1.48 \text{ m}$ ,  $U_g = 0.8 \text{ W/m}^2\text{K}$ ), the resulting curtain wall U-value ( $U_{cw}$ ) is  $1.46 \text{ W/m}^2\text{K}$ . Although above the level of highly insulated systems, this performance may be acceptable for non-residential or yacht applications with less stringent climatic requirements.

An additional simulation showed that adding insulation blocks within the cavity can reduce the  $U_f$  to  $1.5 \text{ W/m}^2\text{K}$  and improve the  $U_{cw}$  to  $1.40 \text{ W/m}^2\text{K}$  (see Fig. 7).

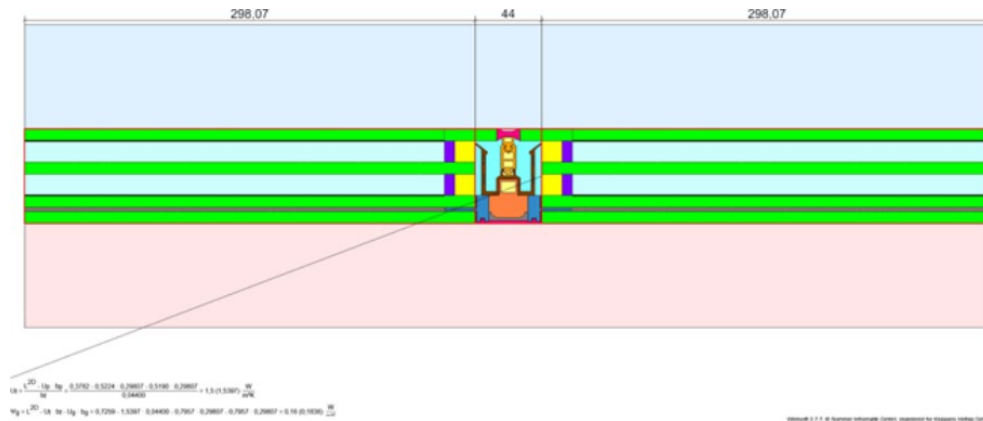


Fig. 7: Illustration of the  $U_f$ -value calculation for triple insulated glazing with insulation blocks in the interspace (Source: knippershelbig).

Condensation simulations according to EN ISO 10211 were conducted for two climate regions. In moderate climates ( $20 \text{ }^\circ\text{C}$ ,  $50 \text{ \% RH}$  inside;  $-5 \text{ }^\circ\text{C}$  outside), no condensation risk was identified, as the dew point isotherm at  $9.3 \text{ }^\circ\text{C}$  lies within the construction (see Fig. 8). Inclined installations proved more critical due to reduced heat flow at corners, where prolonged high humidity ( $>80 \text{ \%}$ ) could promote mold growth. In desert climates ( $43 \text{ }^\circ\text{C}$ ,  $80 \text{ \% RH}$  outside;  $20 \text{ }^\circ\text{C}$  inside), the dew point isotherm at  $38.8 \text{ }^\circ\text{C}$  also remains within the construction without immediate risk; moisture ingress from aged seals would be drained outside the secondary drainage plane.

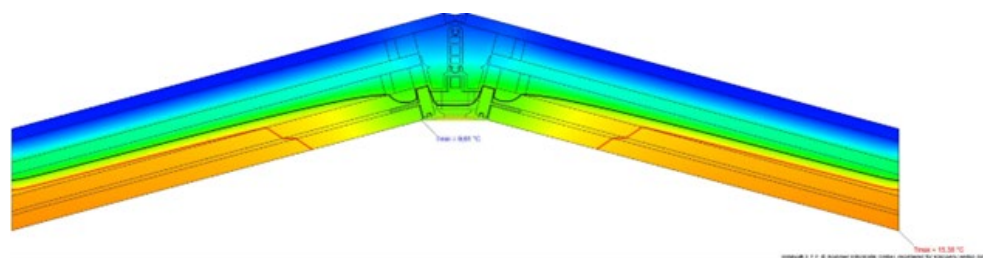


Fig. 8: Illustration of the condensation simulation in temperate climate with triple insulated glazing at inclined installation angles (Source: knippershelbig).

For the double-glazed configuration, the frame U-value is  $2.5 \text{ W/m}^2\text{K}$  (see Fig. 9), again exceeding values of comparable steel façade systems ( $U_f \approx 1.3\text{--}1.8 \text{ W/m}^2\text{K}$ ). With standard roof dimensions ( $1.23 \times 1.48 \text{ m}$ ) and  $U_g = 1.6 \text{ W/m}^2\text{K}$ , the overall  $U_{cw}$  reaches  $2.2 \text{ W/m}^2\text{K}$ . Condensation simulations indicate a risk in temperate climates, where the dew point isotherm intersects interior surfaces (see Fig. 10), making triple glazing preferable. In desert climates, no immediate condensation risk was observed, even for double glazing (Fig. 11).

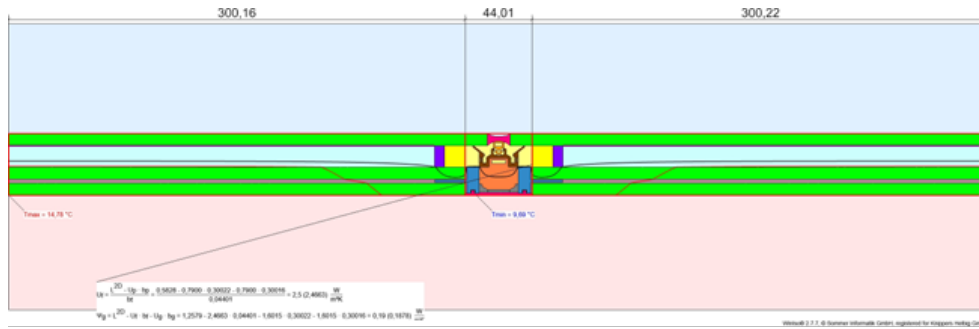


Fig. 9: Illustration of the Uf-value calculation for double insulated glazing (Source: knippershelbig).

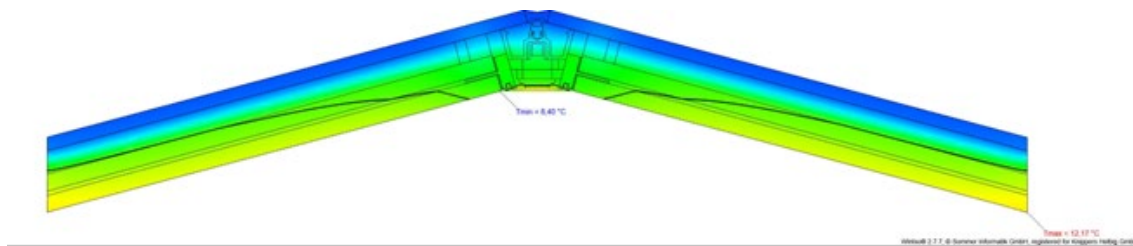


Fig. 10: Illustration of the condensation simulation in a temperate climate with double insulated glazing (Source: knippershelbig).

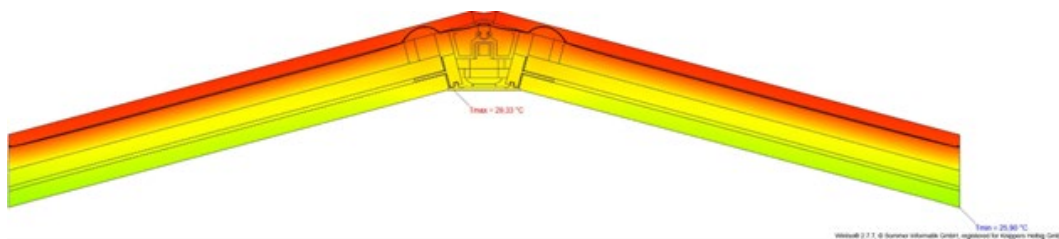


Fig. 11: Illustration of the condensation simulation in desert climate with double insulated glazing (Source: knippershelbig).

Overall, the simulations demonstrate adequate thermal and hygrothermal performance across climate zones, with limitations. While Uf values of 2.0–2.5 W/m<sup>2</sup>K are below those of highly insulated façade systems, insulation blocks can improve performance to 1.5 W/m<sup>2</sup>K. Triple glazing is recommended for temperate climates, whereas double glazing may be sufficient for desert conditions. For the intended applications in non-residential buildings and yachts, the trade-off between thermal efficiency and design flexibility is considered acceptable.

#### 4.2. Solar radiation simulations using COMSOL

In a second step, the thermal behaviour of the FFGC system under solar radiation was analysed using COMSOL Multiphysics to assess temperature distributions within glazing units, steel fittings, and interface zones. Solar heat gain was identified as a critical factor influencing both interior comfort and material stresses, particularly for large glass surfaces and varying orientations.

Three key input parameters defined the simulations: glass composition, climate zone, and pane orientation. Four representative glazing configurations were selected—best- and worst-case scenarios for both double- and triple-insulated glazing—based on common façade practice and

cost-performance considerations. Climate conditions were modelled for five zones: desert, tropical, subtropical, temperate, and cold. The glass orientation ranged from horizontal to vertical, including cardinal directions, strongly affecting heat transfer coefficients (DIN EN ISO 6946) and solar exposure. Based on these parameters, ten simulation models were created, each evaluated in ten variants, resulting in 100 simulations in total. The results were documented systematically. COMSOL generated temperature-distributed data, with particular focus on the interface between steel fitting, glass, and PVB interlayer, where differing thermal expansion coefficients may induce stresses and delamination risk. The simulations enabled robust assessment of thermal loads under realistic conditions (see Fig. 12–13).

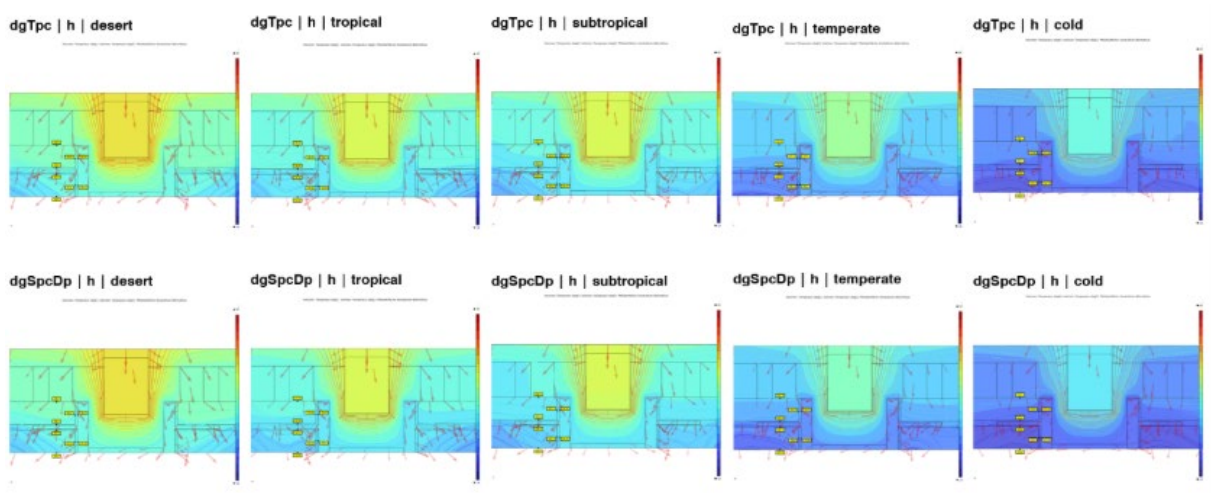


Fig. 12: Simulation results for horizontally oriented double-insulated glazing by climate zone for best- and worst-case scenarios (Source: knippershelbig).

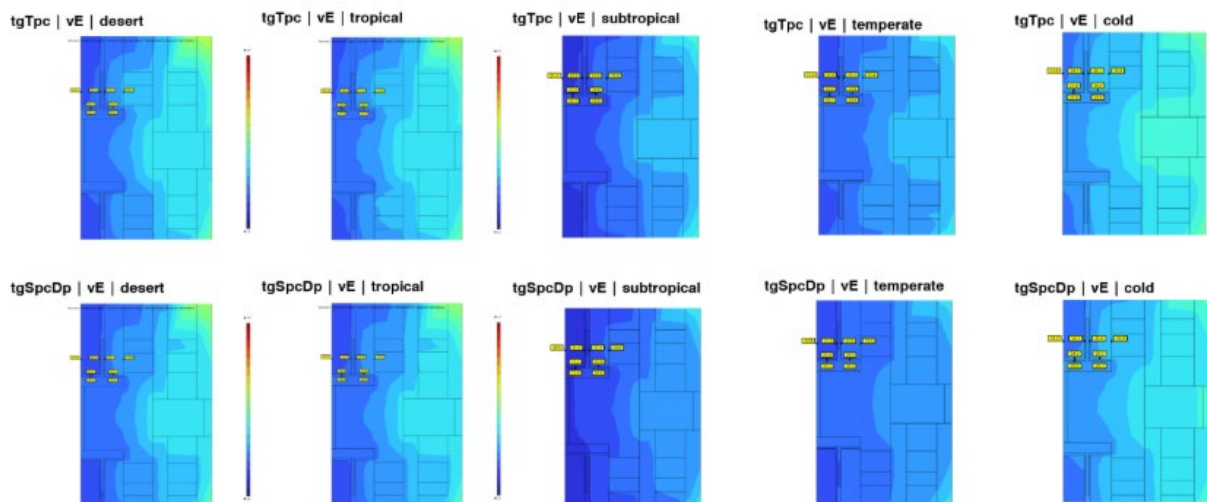


Fig. 13: Simulation results for vertically oriented tripple-insulated glazing facing east by climate zone for best- and worst-case scenarios (Source: knippershelbig).

The complete simulation dataset formed the basis for a Grasshopper-based visualization tool that displays temperature distributions as interactive three-dimensional diagrams (see Fig. 14). These visualizations allow extraction of minimum and maximum temperatures at the critical fitting–PVB interface, which serve as input values for subsequent structural simulations and iterative glazing optimization.

Based on the results, triple-glazed insulating glass is required for cool and temperate climates, whereas double glazing remains feasible in warmer regions. Final glazing selection remains project-specific, balancing building physics, structural, economic, and functional criteria.

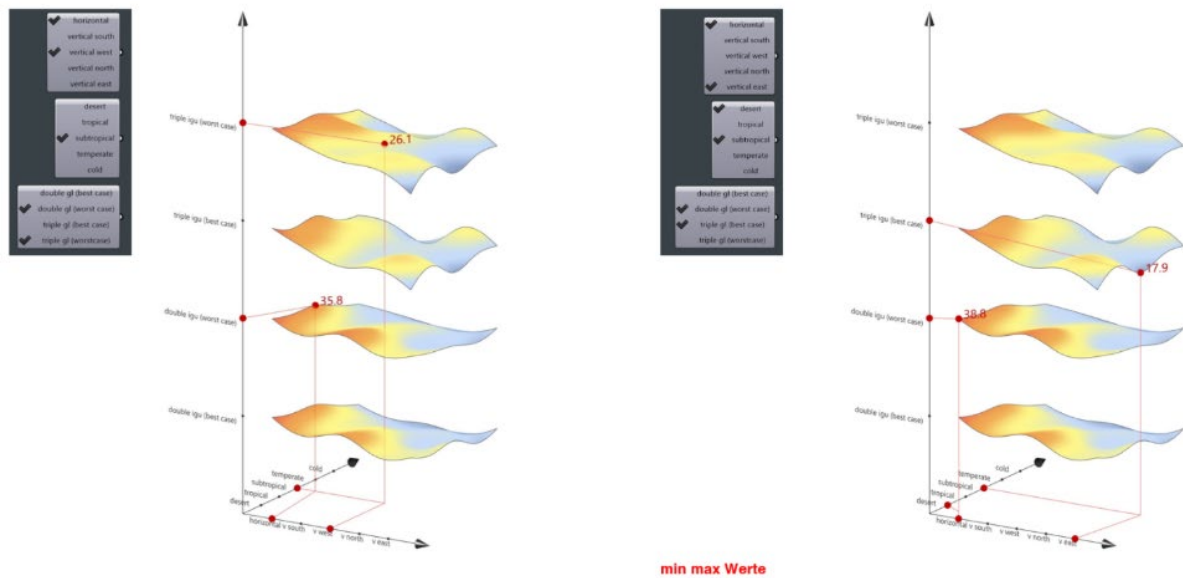


Fig.14: Three-dimensional visualization of simulated temperature distributions as a function of glazing configuration, orientation, and climatic zone, with indicated minimum and maximum temperature values (Source: knippershelbig).

For yacht applications, additional simulations accounted for solar radiation reflected from the water surface. COMSOL analyses of the most critical vertical configurations revealed a temperature increase of approximately 4.5% for both double- and triple-glazed units. This value can be applied as a correction factor to previous results when evaluating maritime use cases.

Together with the building-physics simulations presented in Chapter 1, these investigations define the environmental performance limits of the FFGC system and provide a foundation for testing its geometric and parametric behaviour at architectural scale.

## 5. Parametric Workflows for Frameless Glass Structures

This section focuses on the geometric and parametric aspects of the FFGC system, investigating how panel layouts, joint widths, and fitting geometries can be systematically generated and controlled. Building on the development of the construction detail described in Section 2 and the insights from the building physics simulations in Section 3, this chapter explores the design and fabrication implications of real-scale applications, providing the foundation for automated modeling, assembly planning, and structural analysis of frameless glass structures.

### 5.1. Definition of Geometric and Design Constraints for the FFGC System

An early conclusion derived from the FFGC requirements profile was that exploiting glass as a load-bearing material requires specific global geometries with introduced curvature to ensure structural stability (see Section 2). Tessellated curved surfaces inevitably lead to angle variations between adjacent glass panels, and in free-form geometries each connection becomes unique due to differing fitting angles.

To address this, a selection of glass canopies and façades was analyzed to study design principles and assembly logic. Key parameters such as span, rise, symmetry versus free-form geometry, panel size, and glazing type informed the definition of global constraints, including minimum glass dimensions, allowable angle variation, and joint width.

To limit complexity, the project focused on flat, quadrilateral glass panels; curved glass would have required laminated curved fittings and was therefore excluded. Quadrilateral elements were chosen to maximize transparency by reducing joint density. Analysis indicated that panel sizes below  $1.5 \times 1.5$  m were disadvantageous, while a maximum span of 15 m was established as a guiding parameter. To maintain installation feasibility and building-physics performance, a constant internal joint width of approximately 40 mm was defined (see Fig. 5 and Fig. 6, item 4). Geometric variation was accommodated by limiting the angle between adjacent panels to  $150^\circ$ , allowing the fittings to absorb angular differences while preserving a uniform interior appearance.

### 5.2. Development of a Parametric Framework for Global Geometry Generation

Based on these criteria, a parametric design tool was developed in Grasshopper for Rhino, using translation surfaces to generate globally curved geometries composed exclusively of flat panels. This approach enables controlled variation while ensuring continuity and constructability (see Fig. 15).

The parametric model outputs all data required for automated fabrication workflows (see Section 2.2) and structural analysis (see Section 4.2), including surface representations of glass panes, ordered fitting endpoints, support points, and unitized directional vectors derived from averaged surface normals. These datasets enable the automated generation of 3D fitting geometries based on parameters such as lamination depth, material thicknesses, and connection layout. A key architectural decision embedded in this workflow is a constant internal joint width, ensuring a uniform interior appearance independently of varying panel angles.

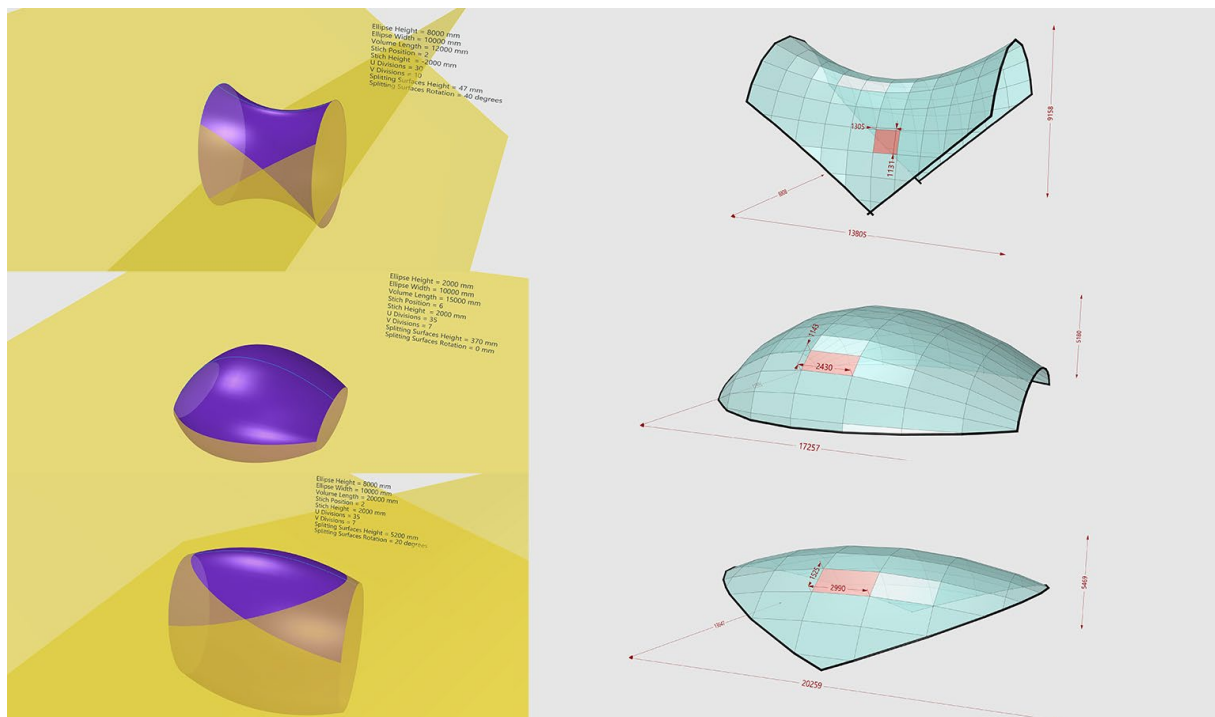


Fig. 15: Examples of geometries produced by the parametric tool (Source: knippershelbig).

Furthermore, both the geometry and the number of connection tabs are parametrically defined based on the spacing between panels resulting from the joint width configuration. The width, length, and thickness of the tabs are controlled by easily adjustable numerical parameters. In this way, the user does not need to draw any geometries manually but only enter numerical values, which automatically generate the corresponding 3D objects with the correct spatial orientation. This parametric approach allows real-time optimization of the design, for example, when feedback from structural analysis indicates the need to increase the number or thickness of linear fittings to improve load transfer. Similarly, the number of screw connections per linear fitting can be flexibly modified to meet structural requirements efficiently.

The structural performance of the frameless glass system was assessed using a multi-scale analysis approach combining globally calibrated models with detailed local investigations. At the global scale, representative roof, façade, and canopy geometries were analysed using parametric finite element models, in which the fitting connections were idealized as translational and rotational springs (see Fig. 16, top). The stiffness parameters were derived from analytical studies, numerical simulations, and validation tests, allowing realistic representation of connection behaviour within the global structural system (Ayvaz et al., 2025). This methodology enabled efficient evaluation of global deformations, force redistribution, stability, and sensitivity to parameters such as temperature, element size, curvature, and load duration.

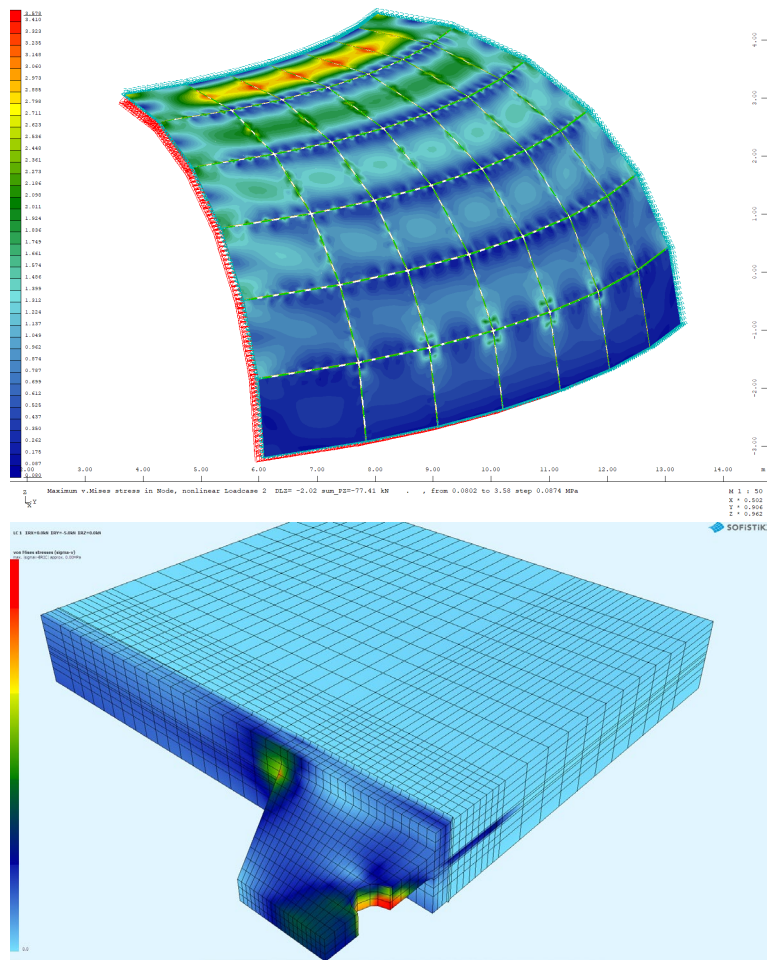


Fig. 16: Van-Mises-Stress results of parametric global (top) and local (bottom) structural FE simulations (Source: Technische Universität Darmstadt ISM+D).

To complement the global analyses, detailed three-dimensional FE models were developed to study stress distributions and potential failure mechanisms within the Fitting–Foil–Glass Composite. These models captured the interaction between steel fitting, interlayer, and glass, identifying critical stress concentrations under normal force, bending, and shear (see Fig. 16, bottom). The combined global–local strategy was essential to assess both system-level behavior and local limit states, including temperature-dependent interlayer stiffness and damage scenarios. The results confirm that spring-based global models provide a reliable assessment, provided their parameters are derived from experimentally validated local analyses.

### 5.3. Development of Parametric Tools for Assembly Automation of Frameless Glass Structures

As described in Section 4.2, an essential aspect of designing and assembling Frameless Glass Structures is the need to work with geometrically distinct glass elements and varying angles between these elements. These variations in geometry and angle require that all components for fabrication and assembly be correctly identified to ensure accurate lamination and proper assembly of the entire structure. The logic behind the identification concept was developed through a closely coordinated, collaborative process involving all project partners.

This logic was also tested during the assembly of a mock-up exhibited at the Glasstec fair in Düsseldorf in 2024. The mock-up was designed as part of a shell structure generated from a translational surface,

servicing both as a demonstration of a full-scale architectural application of the developed FFGC system and as a test of the newly developed fabrication method for the fittings (see Fig 17 - 18). The dimensions of the mock-up comprise a span of approximately 6.7 m, a rise of 1.9 m, and a width of 3.3 m, with the longest fitting measuring about 2.2 m in length.



Fig. 17: Real-scale architectural prototype for the Glasstec fair in Düsseldorf, 2024 (Source: knippershelbig).



Fig. 18: Close-up of the construction detail and fittings produced for the Glasstec mock-up exhibited in Düsseldorf in 2024 (Source: knippershelbig).

To establish an appropriate identification system, an assembly sequence was first defined. This sequence depended primarily on the arrangement of the fittings (top or bottom). In practical applications, a rectangular element may have between two and four neighbouring elements, depending on the boundary conditions (see Fig. 19). Thus, it is crucial to consider the position of the fittings on all adjacent elements to avoid collisions during assembly. This is directly related to the sequence in which the finished glass elements are placed. Once the sequence for the Glasstec prototype was defined, each glass element was assigned an identification number, shown in Fig. 20 as an example from 1 to 8. For the lamination process, the identification number of each fitting must include information about the glass element to which it belongs, the neighbouring element it connects

to, and whether its tabs are positioned at the top or bottom. This information serves two purposes: first, to enable double-checking during fabrication and ensure accuracy; second, to assist assembly by clearly indicating which element is placed on top of which. The parametric tool for assembly generated these labels automatically by calculating which edges were shared by which neighbouring elements, ensuring consistency and reducing the risk of errors during fabrication and installation.

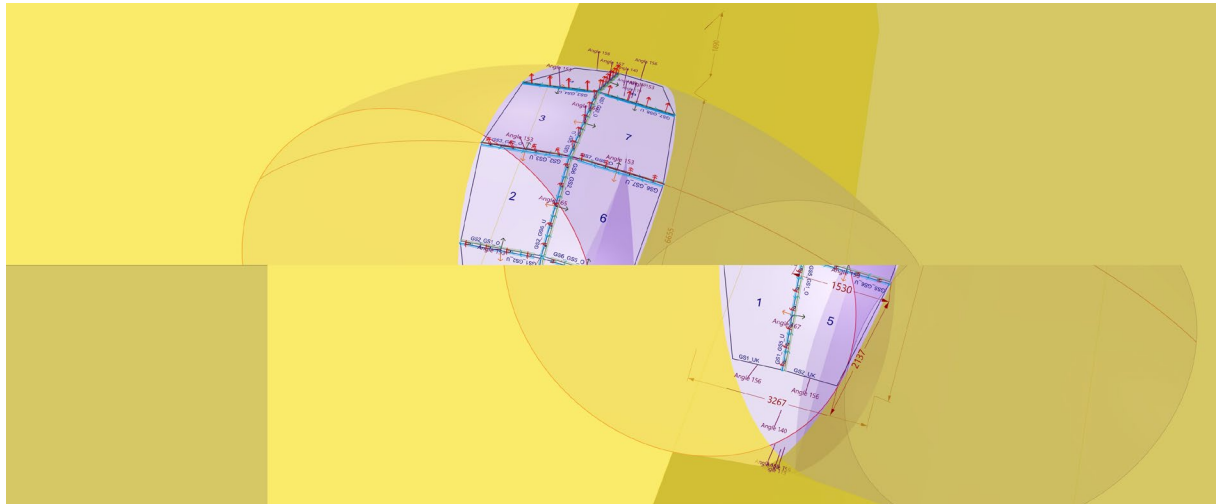


Fig. 19: Global geometry model and corresponding assembly sequence for the Glasstec mock-up exhibited in Düsseldorf in 2024 (Source: knippershelbig).



Fig. 20: Close-up of the labelling system, produced by the parametric tool for the assembly of the Glasstec mock-up exhibited in Düsseldorf in 2024 (Source: knippershelbig)

Once the fittings and glass surfaces are generated in 3D, the tool automatically lays them flat on the XY-world plane with the correct labels positioned beside them—ready for the automated creation of fabrication drawings. These drawings are then forwarded to the steel manufacturer responsible for producing the fittings. Each fitting is engraved with identification numbers in two locations – at the part laminated in between the glass panes (see Fig. 21, left) and at the backside of the T-Profile (see Fig. 21, right). This method streamlines both the lamination process and the subsequent assembly. At every stage of production, the sequence and orientation of each fitting can be verified, ensuring accurate, efficient, and seamless lamination and assembly of the structure.

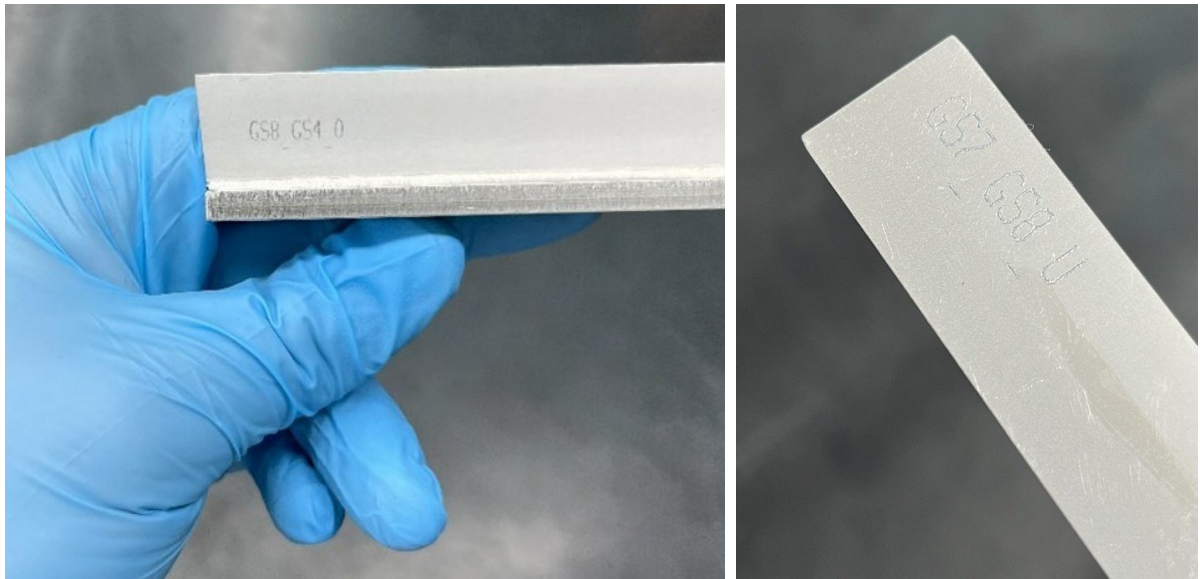


Fig. 21: Examples for the engraved identification number on two sides of a fitting (Source: Yachtglass).

The systematic approach to identifying, labelling, and assembling glass elements and fittings not only ensures accuracy during fabrication and installation but also provides a clear basis for quantifying material use and manufacturing requirements. By establishing precise information on the geometry, number, and position of each component, as well as the associated fittings and lamination processes, the workflow generates the data necessary for evaluating the environmental impacts of the entire system. These parameters form the foundation for the subsequent life cycle assessment, allowing a detailed analysis of the embodied carbon, material consumption, and potential environmental benefits of the investigated frameless glass construction system.

## 6. Life-Cycle-Assessment Tool for Frameless Glass Structures

Within the framework of this research project, a Life Cycle Assessment (LCA) was conducted for the developed FFGC system in accordance with ISO 14040 and ISO 14044. The system boundaries followed a cradle-to-grave approach, covering life-cycle stages A to C. The analysis included stages A1–A3 (raw material supply, transport, and manufacturing) and C3–C4 (waste processing and disposal). Stages A4–A5, B, and C1–C2 were excluded, as their evaluation would require project-specific data. The study is therefore project-independent; a complete LCA would require adding these stages separately.

The assessment considered all major components of the FFGC system, including glazing, linear fittings, local connections, wet silicone joints, backing rods, and dry seals, each evaluated using appropriate reference units. Manufacturer-specific and generic datasets were collected, and average Global Warming Potential (GWP) values were derived to improve robustness. Dataset reference units were converted to consistent reference units.

Particular emphasis was placed on glazing, with multiple manufacturer datasets compared. GWP values were differentiated for individual panes based on thickness, coatings, tempering processes, recycled content, and double or triple glazing configurations, enabling parametric evaluation of customized glazing assemblies.

The resulting GWP values were integrated into a Grasshopper-based parametric geometric model, allowing automated mass calculations across design variants. Total CO<sub>2</sub>-equivalent emissions were determined by combining component masses with their respective GWP values (Fig. 22).

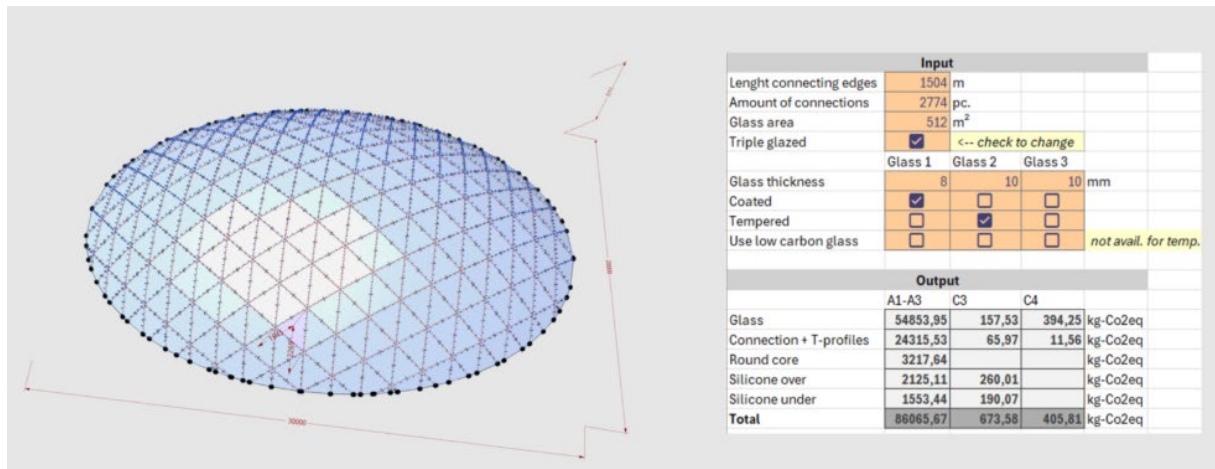


Fig. 22: CO<sub>2</sub> emission results from the integration of the parametric geometric model with an automated Excel-based LCA tool (Source: knippershelbig).

For comparison, an LCA was conducted for a conventional steel-based system consisting of a steel substructure with rectangular hollow sections (50 × 125 mm), add-on construction, and glazing. The results show that the frameless glass construction reduces CO<sub>2</sub>-equivalent emissions by approximately 55% relative to the reference system, demonstrating its significant ecological potential.

Future research should extend the analysis to project-specific life-cycle stages and operational phases to enable a complete LCA and further support design-integrated environmental optimization.

## 7. Results and conclusions

This research successfully developed an integrated workflow for frameless glass structures that addresses fabrication feasibility, thermal performance, parametric automation, environmental impact, and real-scale validation, demonstrating that glass can function as a true load-bearing material while maintaining thermal envelope integrity.

The iterative prototyping process established a viable fabrication method using laser-welded stainless-steel components, significantly reducing costs compared to CNC milling. However, challenges in welding consistency—particularly maintaining uniform seam thickness and preventing heat-induced deformation—directly impacted lamination quality and revealed a critical finding: achieving desired performance requires much tighter integration between design and manufacturing partners, with steel fabricators ideally included in the core project team. These fabrication sensitivities informed the thermal analysis, where comprehensive COMSOL simulations across 100 scenarios generated a robust database of thermal behavior at the critical fitting-glass-PVB interface. Triple-glazed configurations achieved frame U-values of up to 1.5 W/m<sup>2</sup>K, with condensation analysis confirming triple glazing is essential for temperate climates while double glazing suffices in desert conditions. An interactive Grasshopper visualization tool integrating these findings enables designers to optimize configurations based on specific boundary conditions, creating direct feedback between environmental performance and structural design.

This simulation-driven approach informed the parametric workflow that automates geometry generation, fabrication data, and assembly logic. By constraining the system to flat quadrilateral panels with angles limited to 150° and uniform 40 mm internal joints, the methodology balances architectural expression with manufacturing feasibility. The comprehensive identification system translated directly into successful assembly of the Glasstec 2024 demonstrator—a 6.7-meter span mock-up that validated technical feasibility while exposing manufacturing precision sensitivities. Most significantly, the Life Cycle Assessment revealed approximately 55% CO<sub>2</sub>-equivalent emission reduction compared to conventional steel-grid systems, demonstrating that transparency and sustainability reinforce rather than compromise one another.

The research establishes that frameless glass architecture can advance toward viable building practice when fabrication, thermal performance, parametric automation, and environmental assessment develop in concert. Future work should explore curved fittings, refine fabrication through automated welding, conduct long-term durability testing, and develop standardized details to accelerate market adoption. The integrated workflow provides a scalable foundation demonstrating that glass structures can achieve both architectural ambition and technical viability.

## Acknowledgements

The authors would like to thank the external partners, who made the Glasstec prototype possible. These are: MVK Heek (Germany), Heavydrive (Germany), Tausch (Netherlands).

Additionally, special thanks go to Paula Elizabeth Esquinca, Dima Othman, Alva Fjallaker, and August Johannesson from knippershelbig, who supported the research and development of the project.

This research project was funded by the Federal Ministry for Economic Affairs and Climate Action based on a resolution of the German Bundestag.

## References

- Arch Daily. (25. 11 2025). Arch Daily. Von Arch Daily: <https://www.archdaily.com/925305/apple-store-fifth-avenue-foster-plus-partners> abgerufen
- Ayvaz, I., Peters, T., Fildhuth, T., Rusenova, G., Buksak, A., Haller, M., . . . Kraus, M. (2025). Structural performance of linearly laminated metal fittings for frameless glass shell structures. *Glass Structures & Engineering*. doi:<https://doi.org/10.1007/s40940-025-00312-4>
- BauNetz. (25. 11 2025). BauNetz. Von BauNetz: <https://www.baunetzwissen.de/glas/objekte/bildung/glasdach-der-mensa-der-tu-dresden-71502> abgerufen
- Detail. (30. 04 2001). Detail. Von Detail: [https://www.detail.de/de\\_en/maximilian-museum-in-augsburg-15670](https://www.detail.de/de_en/maximilian-museum-in-augsburg-15670) abgerufen
- Deutsches Institut für Normung (DIN). (2015). DIN EN 12150-1:2015-12 Glass in building - Thermally toughened soda lime silicate safety glass - Part 1: Definition and description;. Deutsches Institut für Normung.
- European Committee for Standardization (CEN). (2005). EN 1993-1-1: Eurocode 3 – Design of steel structures – Part 1-1: General rules and rules for buildings. Brussels: CEN.
- European Committee for Standardization (CEN). (2011). EN 15978: Sustainability of construction works – Assessment of environmental performance of buildings – Calculation method. Brussels: CEN.
- European Committee for Standardization (CEN). (2019). EN 15804+A2: Sustainability of construction works – Environmental product declarations – Core rules for the product category of construction products. Brussels: CEN.
- Fildhuth, T. (2022). Design Base for a Frameless Glass Structure Using Structural PVB Interlayers and Stainless-Steel Fittings. doi: <https://doi.org/10.47982/cgc.8.369>
- Intelligence, M. (25. 11 2025). Mordor Intelligence. Von Mordor Intelligence: <https://www.mordorintelligence.com/industry-reports/europe-luxury-yacht-market> abgerufen

- knippershelbig. (25. 11 2025). knippershelbig. Von knippershelbig: <https://www.knippershelbig.com/projekte/eastman-rahmenlose-glasstruktur-messestand/> abgerufen
- Marinitsch, S. (2015). Stabilitätsprobleme bei faltwerken aus Glas [Dissertation, Technische Universität Wien]. reposiTUm.
- Salim, A. (25. 11 2025). Ibis World. Von Ibis World: <https://www.ibisworld.com/germany/industry/flat-glass-manufacturing/762/#KeyStatistics> abgerufen
- Seele. (25. 11 2025). Seele. Von Seele: <https://seele.com/project/glass-roof> abgerufen
- Sobek, W., & Blandini, L. (2004). Prototype of a frameless structural glass shell. Shell and Spatial Structures from Models to Realization. Madrid: Montpellier.

## Platinum Sponsor

---



## Gold Sponsors

---



## Silver Sponsors

---



## Organisation

---

